Simplified Numerical Analysis of Suspension Bridges

Diego Cobo del Arco and Angel C. Aparicio, *Technical University of Catalonia, Spain*

Discretization methods are widely used in the analysis and design of suspension bridges. However, the large number of variables involved do not normally allow examination of the influence of different parameters on the behavior of suspension bridges. This paper presents a numerical method of analysis of suspended cables under vertical loads. Both explicit equilibrium and tangent stiffness matrices are derived by the finite element method. The expressions are also presented in dimensionless form, so that parametric studies can be performed. The obtained matrices can be assembled easily in a general structural analysis computer program. The proposed method is applied to the simplified analysis of suspension bridges. Some dimensionless charts are given for a single span suspension bridge. These include displacement and bending moments under the position of a concentrated load, pseudoinfluence line of displacement and bending moments at the quarter of span, and maximum displacements and bending moments for an arbitrarily located distributed load. It is believed that these charts can be useful in the first phase of design of suspension bridges and can contribute to the understanding of suspension bridge behavior.

Suspension bridges are flexible structures where geometric nonlinear analysis must be performed in order to include the stiffening effect of the tension in the cable.

Various methods of analysis have been applied to the study of the behavior of suspension bridges. A historical review of the approximate methods that lead to the deflection theory can be found elsewhere (*1*,*2*). The well-established deflection theory (*2*–*4*) tries to solve the differential equilibrium equation and allows the use of analytical expressions for the solutions. However, explicit analytical solutions are not always possible, and numerical techniques must be used (*2*,*5*).

On the other hand, discretization methods have been widely used in the modern design and analysis of suspension bridges, both in the static and the dynamic fields (e.g., *6*–*9*). Normally this leads to problems where the number of unknowns is very large (*9*). It is difficult, then, to examine the influence of different parameters on the behavior of the suspension bridge.

This paper presents a numerical method of analysis of suspended cables under vertical loads. The finite element method is used to obtain an explicit stiffness matrix, where the different nonlinear terms are readily identified. The equations are also presented in their nondimensional form (*5*). Parametric studies can then be performed. This stiffness matrix can be assembled in a general computer program.

The proposed method is applied to the analysis of suspension bridges. Two parameters govern the behavior of the single-span suspension bridge. Some dimensionless charts are developed as a function of these two

parameters for a single-span suspended bridge. These charts include displacement and bending moment under the position of a concentrated load, pseudoinfluence lines for displacement and bending moments at the quarter of span, and maximum displacement and bending moments for an arbitrarily located distributed load.

Governing Equations

According to Figure 1, q_0 is the load per unit of horizontal length in the reference configuration, and H is the horizontal force in the cable. The vertical equilibrium equation reads (*5*)

$$H\frac{d^2z}{dx^2} = -q_0 \qquad z(0) = 0 \qquad z(l) = 0 \tag{1}$$

Under the action of additional load $q(x)$ and rise of temperature t, the cable deforms from the reference configuration. The differential equations of equilibrium are (*5*)

$$\left.\begin{aligned} &H\frac{d^2w}{dx^2} + h\left(\frac{d^2z}{dx^2} + \frac{d^2w}{dx^2}\right) = -q \\ &V_A = -(H+h)\left(\frac{dw}{dx}\right)_A - h\left(\frac{dz}{dx}\right)_A \\ &V_B = (H+h)\left(\frac{dw}{dx}\right)_B + h\left(\frac{dz}{dx}\right)_B \end{aligned}\right\} \tag{2}$$

$$\frac{dh}{dx} = 0 \qquad F_A = -h_A \,. \quad F_B = h_B \tag{3}$$

V_A, V_B, F_A, F_B are the increment in reaction forces at ends A and B with the signs of Figure 2. Equations 2 and 3 assume that $du/dx << 1$ where $u(x)$ is the horizontal movement.

The increment in horizontal force h can be obtained from the compatibility equation. This equation, up to the second order, is given by

$$h = \frac{EA}{L_e}\left[u_B - u_A + \left(\frac{dz}{dx}\right)_B w_B - \left(\frac{dz}{dx}\right)_A w_A + \frac{q_0}{H}\int_A^B w\,dx + \frac{1}{2}\int_A^B \left(\frac{dw}{dx}\right)^2 dx\right] - \frac{EA\alpha t L_t}{L_e} \tag{4}$$

where E is the elastic modulus, A is the cross-sectional area of the cable, α is the thermal expansion coefficient, and L_e and L_t are defined as

$$L_e = \int_A^B \left(\frac{dS_R}{dx}\right)^3 dx \qquad L_t = \int_A^B \left(\frac{dS_R}{dx}\right)^2 dx \tag{5}$$

For the particular case of supports and at the same level, it is commonly accepted that

$$L_e = \left[1 + 8\left(\frac{f}{l}\right)^2\right] l \qquad L_t = \left[1 + \frac{16}{3}\left(\frac{f}{l}\right)^2\right] l \tag{6}$$

f being the sag in the cable (Figure 1). Equations 1 through 6 are valid as long as only vertical loads are applied. These include cases such as Figure 1, but also cases such as Figure 2, where reactions at intermediate points are treated as external vertical forces.

The virtual work principle for the cable can be obtained from Equations 2 and 3. Considering a cable be-

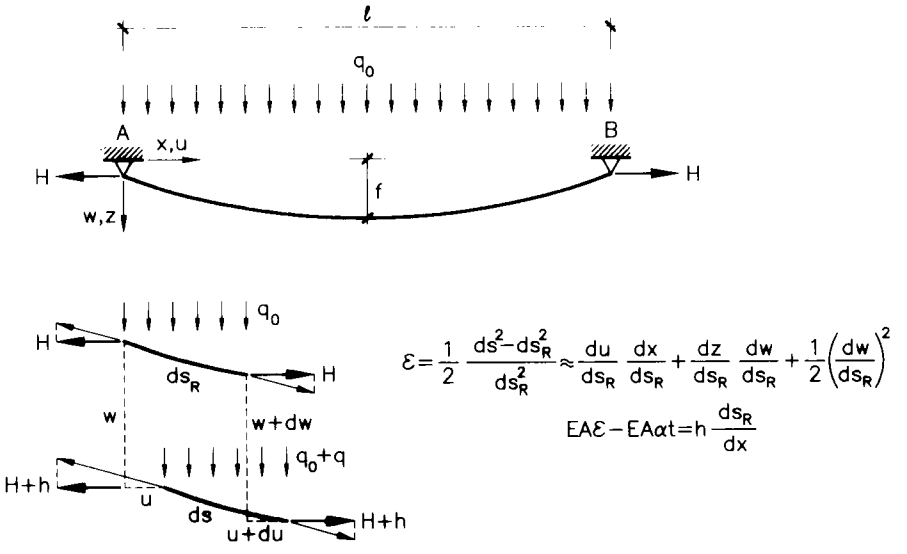

FIGURE 1 Reference and deformed configuration under vertical load.

FIGURE 2 Definition of forces at ends of cable.

tween points A and B, let F_A, F_B, V_A, V_B be the increments in forces at the ends of the cable (see Figure 2). Let Equation 2 be multiplied by an arbitrary function $\delta w(x)$ and let Equation 3 be multiplied by an arbitrary function $\delta u(x)$. Using Equation 1, integrating the equations and adding them yields (*10*)

$$H\int_A^B \frac{dw}{dx}\frac{d\delta w}{dx}\,dx + h\int_A^B \frac{dw}{dx}\frac{d\delta w}{dx}\,dx + h \times \left[\frac{q_0}{H}\int_A^B \delta w dx + \delta u_B - \delta u_A + \left(\frac{dz}{dx}\right)_B \delta w_B - \left(\frac{dz}{dx}\right)_A \delta w_A\right] = F_A\delta u_A + F_B\delta u_B + V_A\delta w_A + V_B\delta w_B + \int_A^B q\delta w dx \quad (7)$$

This is the virtual work principle for the cable. The last term of the right-hand side should include the term $\Sigma q_i \delta w_i$ when concentrated vertical loads q_i are applied.

Finite Element Model

A simple finite element model can be obtained from Equations 4 and 7. Let the cable between points A and B be discretized into n parts, each of horizontal length l_i (Figure 3).

Linear displacements are assumed between nodes i and $i + 1$. This leads to dw/dx being discontinuous between nodes,which actually occurs when a concentrated load acts at a particular node. Defining,

$$\mathbf{d}^t = (u_1, w_1, w_2, \ldots, w_n, w_{n+1}, u_{n+1}) \quad (8)$$

$$\boldsymbol{\delta}\mathbf{d}^t = (\delta u_1, \delta w_1, \delta w_2, \ldots, \delta w_n, \delta w_{n+1}, \delta u_{n+1}) \quad (9)$$

it is possible to express

$$\int_A^B \frac{dw}{dx}\frac{d\delta w}{dx}\,dx = \boldsymbol{\delta}\mathbf{d}^t \cdot \underline{\underline{C}} \cdot \mathbf{d} \quad (10)$$

$$u_B - u_A + \left(\frac{dz}{dx}\right)_B w_B - \left(\frac{dz}{dx}\right)_A w_A + \frac{q_0}{H}\int_A^B w dx = \mathbf{a}^t \cdot \mathbf{d} \quad (11)$$

where $\mathbf{a}$ is a vector whose dimension is $(n + 3)$ and $\underline{\underline{C}}$ is a symmetric matrix whose dimension is $(n + 3)x(n + 3)$. The explicit expressions for $\mathbf{a}$ and $\underline{\underline{C}}$ can be found in Tables 1 and 2, respectively.

Introducing Equations 10 and 11 in Equation 4, Equation 12 is written

$$h = \frac{EA}{L_e}\left(\mathbf{a}^t \cdot \mathbf{d} + \frac{1}{2}\mathbf{d}^t \cdot \underline{\underline{C}} \cdot \mathbf{d}\right) - EA\alpha t\frac{L_t}{L_e} \quad (12)$$

Introducing Equations 10 and 11 in Equation 7, after manipulations, the virtual work principle is being given by

$$\boldsymbol{\delta}\mathbf{d}^t \cdot [H\underline{\underline{C}} \cdot \mathbf{d} + h(\mathbf{a} + \underline{\underline{C}} \cdot \mathbf{d})] = \boldsymbol{\delta}\mathbf{d}^t \cdot (\mathbf{F} + \Sigma\mathbf{q}_i) \quad (13)$$

As Equation 13 holds for every virtual displacement $\boldsymbol{\delta}\mathbf{d}$, it is possible to write the equation of equilibrium as

$$H\underline{\underline{C}} \cdot \mathbf{d} + h(\mathbf{a} + \underline{\underline{C}} \cdot \mathbf{d}) - \Sigma\mathbf{q}_i = \mathbf{F} \quad (14)$$

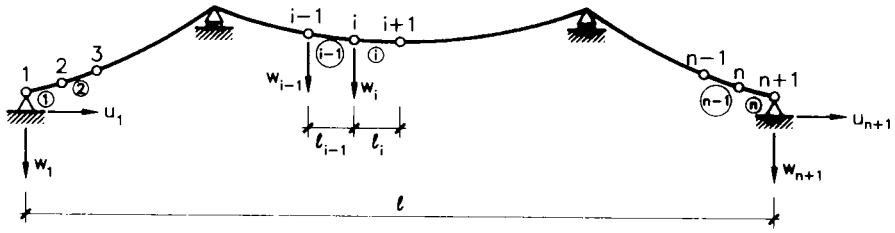

FIGURE 3 Finite element discretization.

TABLE 1 Expression for Vector a

	u_1	w_1	w_2	...	w_i	...	w_n	w_{n+1}	u_{n+1}
i	1	2	3		i+1		n+1	n+2	n+3
a_i	-1	$-Z'_A + q_0 l_1/2H$	$q_0(l_1+l_2)/2H$		$q_0(l_i+l_{i-1})/2H$		$q_0(l_n+l_{n-1})/2H$	$Z'_B + q_0 l_n/2H$	1

Equation 13 is a typical finite element equilibrium equation (*11*). **F** is the internal force vector at the ends of the element and $\Sigma \mathbf{q}_i$ is the external force vector, although $\Sigma \mathbf{q}_i$ could be interpreted as internal forces if the cable is a part of a general structure. Introducing Equation 12 in Equation 14, an equilibrium stiffness matrix (*12*) can be readily identified:

$$\underline{\underline{K}}_e \cdot \mathbf{d} - EA\alpha t \frac{L_t}{L_e} \mathbf{a} - \Sigma \mathbf{q}_i = \mathbf{F} \tag{15}$$

$$\underline{\underline{K}}_e = \frac{EA}{L_e} \mathbf{a} \cdot \mathbf{a}^t + \left(H + \frac{1}{2} h^1 + \frac{1}{3} h^2 - EA\alpha t \frac{L_t}{L_e}\right) \underline{\underline{C}} + \frac{EA}{L_e}\left[\frac{1}{2} (\mathbf{a} \cdot \mathbf{d}^t \cdot \underline{\underline{C}} + \underline{\underline{C}} \cdot \mathbf{d} \cdot \mathbf{a}^t) + \frac{1}{3} \underline{\underline{C}} \cdot \mathbf{d} \cdot \mathbf{d}^t \cdot \underline{\underline{C}}\right] \tag{16}$$

where the increment in horizontal force h is obtained as the sum of the first-order contribution h^1 and the second-order contribution h^2, which are given by

$$\left.\begin{aligned} h^1 &= \frac{EA}{L_e} \mathbf{a}^t \cdot \mathbf{d} \\ h^2 &= \frac{1}{2} \frac{EA}{L_e} \mathbf{d}^t \cdot \underline{\underline{C}} \cdot \mathbf{d} \\ h &= h^1 + h^2 - EA\alpha t \frac{L_t}{L_e} \end{aligned}\right\} \tag{17}$$

Equation 15 gives an explicit equilibrium stiffness matrix for the whole cable under vertical loads. It is of interest to note that the structure of Equation 15 is the same as in a total Lagrangian geometrically nonlinear analysis (*12*). Thus, differentiating Equation 14, the tangent stiffness matrix for the whole cable is obtained straighforwardly and given by

$$\underline{\underline{K}}_t = \frac{EA}{L_e} \mathbf{a} \cdot \mathbf{a}^t + \left(H + h^1 + h^2 - EA\alpha t \frac{L_t}{L_e}\right) \underline{\underline{C}} + \frac{EA}{L_e} (\mathbf{a} \cdot \mathbf{d}^t \cdot \underline{\underline{C}} + \underline{\underline{C}} \cdot \mathbf{d} \cdot \mathbf{a}^t + \underline{\underline{C}} \cdot \mathbf{d} \cdot \mathbf{d}^t \cdot \underline{\underline{C}}) \tag{18}$$

The first term of the expression 18 can be regarded as the linear contribution, the second term is the initial stress matrix, and the third term is the initial displacement matrix (*12*). This tangent stiffness matrix can be used to perform an analysis with a Newton-Raphson scheme (*11*). The residual vector can be evaluated with either Equation 14 or 15.

Dimensionless Equations

All the equations presented can be put in dimensionless terms, as shown by Irvine (*5*). Defining the nondimensional variables,

$$\left.\begin{aligned} x' &= \frac{x}{l} \qquad h' = \frac{h}{H} \qquad \mathbf{d}' = \frac{H}{q_0 l^2} \mathbf{d} \\ \mathbf{q}' &= \frac{1}{q_0 l} \mathbf{q} \qquad \theta = \frac{\alpha t L_t}{\frac{HL_e}{EA}} \qquad \lambda^2 = \left(\frac{q_0 l}{H}\right)^2 \frac{l}{\frac{HL_e}{EA}} \end{aligned}\right\} \tag{19}$$

where l is a characteristic length of the cable (see, for example, Figure 1 or Figure 3), it is possible to derive

$$\underline{\underline{K}}'_e \cdot \mathbf{d}' - \theta \mathbf{a}' - \Sigma \mathbf{q}' = \mathbf{f}' \tag{20}$$

$$\underline{\underline{K}}'_e = \lambda^2 \mathbf{a}' \cdot \mathbf{a}'^t + (1 + \frac{1}{2} h^{1\prime} + \frac{1}{3} h^{2\prime} - \theta) \underline{\underline{C}}' + \lambda^2 \left[\frac{1}{2} (\mathbf{a}' \cdot \mathbf{d}'^t \cdot \underline{\underline{C}}' + \underline{\underline{C}}' \cdot \mathbf{d}' \cdot \mathbf{a}'^t) + \frac{1}{3} \underline{\underline{C}}' \cdot \mathbf{d}' \cdot \mathbf{d}'^t \cdot \underline{\underline{C}}'\right] \tag{21}$$

$$\underline{\underline{K}}'_t = \lambda^2 \mathbf{a}' \cdot \mathbf{a}'^t + (1 + h^{1\prime} + h^{2\prime} - \theta) \underline{\underline{C}}' + \lambda^2 (\mathbf{a}' \cdot \mathbf{d}'^t \cdot \underline{\underline{C}}' + \underline{\underline{C}}' \cdot \mathbf{d}' \cdot \mathbf{a}'^t + \underline{\underline{C}}' \cdot \mathbf{d} \cdot \mathbf{d}'^t \cdot \underline{\underline{C}}') \tag{22}$$

$$\left.\begin{aligned} h^{1\prime} &= \lambda^2 \mathbf{a}'^t \cdot \mathbf{d}' \qquad h^{2\prime} = \frac{1}{2} \lambda^2 \mathbf{d}'^t \cdot \underline{\underline{C}}' \cdot \mathbf{d}' \\ h' &= h^{1\prime} + h^{2\prime} - \theta \end{aligned}\right\} \tag{23}$$

TABLE 2 Expression for Matrix $\underline{\underline{C}}$

$\underline{\underline{C}}$		u_1	w_1	w_2	w_3	...	w_{n-1}	w_n	w_{n+1}	u_{n+1}
		1	2	3	4		n	n+1	n+2	n+3
u_1	1	0	0	0	0	0	0	0	0	0
w_1	2	0	$1/l_1$	$-1/l_1$	0	0	0	0	0	0
w_2	3	0	$-1/l_1$	$1/l_1+1/l_2$	$-1/l_2$	0	0	0	0	0
w_3	4	0	0	$-1/l_2$	$1/l_2+1/l_3$	...	0	0	0	0
...	...	0	0	0	...	...	...	0	0	0
w_{n-1}	n	0	0	0	0	...	$1/l_{n-2}$ $+1/l_{n-1}$	$-1/l_{n-1}$	0	0
w_n	n+1	0	0	0	0	0	$-1/l_{n-1}$	$1/l_{n-1}$ $+1/l_n$	$-1/l_n$	0
w_{n+1}	n+2	0	0	0	0	0	0	$-1/l_n$	$1/l_n$	0
u_{n+1}	n+3	0	0	0	0	0	0	0	0	0

$$\mathbf{a}' = \frac{H}{q_0 l}\,\mathbf{a} \qquad \underline{\underline{C}}' = l\underline{\underline{C}} \tag{24}$$

The expressions for $\mathbf{a}'$ and $\underline{\underline{C}}'$ are extremely simple when the cable is discretized in n equal parts and can be obtained easily from the values of Tables 1 and 2.

Equations 19 through 23 can be very useful when performing a parametric investigation. The behavior of the cable is uniquely described by λ^2 and the values of the nondimensional loads q'. Parameter λ^2 has been interpreted by Irvine (*5*). It accounts for the relation between geometric and elastic stiffness. It is small for taut flexible cables and it approaches infinity for an inextensible suspended cable. Typical values for λ^2 in suspension bridge cables lie in the range 100 to 400 (*5*). Effectively, for the usual ratio f/l = 0.1 in a steel suspension bridge cable and for a service stress σ about 500 MPa, the value of λ^2 is on the order of 250. On the other hand, typical values for nondimensional concentrated loads are on the order of 0.01 in suspension bridges because of the large dead load. As an example, for the George Washington Bridge, neglecting the side spans, λ^2 = 255, and for a concentrated load of 1000 kN, the value of q' is as low as 0.0016 [data are taken from Buonopane and Billington (*1*) for the George Washington Bridge as originally built].

The nondimensional approach can be used to examine the accuracy of the proposed method of analysis. Table 3 shows the vertical displacements in the center of the span of a suspended cable with supports at the same level under a central concentrated load q' = 1.0 Whereas the values chosen for λ^2 are typical of suspension bridge cables, the value chosen for q' is extremely high. It is seen in Table 3 that even for a small number of discretization points the accuracy obtained is high.

The previously derived formulation can be used directly to obtain the solution for the inextensible cable. From Equation 14, the displacements $\mathbf{d}'$ in dimensionless form are given by

$$\mathbf{d}' = \frac{1}{1 + h'}\,\underline{\underline{C}}'^{-1} \cdot (\Sigma \mathbf{q}_i' - h'\mathbf{a}') \tag{25}$$

TABLE 3 Accuracy of Proposed Method of Analysis

	w ' λ^2=100	h ' λ^2=100	w ' λ^2=200	h ' λ^2=200	w ' λ^2=400	h ' λ^2=400
n+1=11	0.0371	1.314	0.0280	1.450	0.0226	1.541
n+1=21	0.0374	1.310	0.0284	1.445	0.0230	1.534
n+1=40	0.0374	1.308	0.0285	1.443	0.0231	1.532
Irvine [9]	0.0375	1.308	0.0285	1.443	0.0231	1.532

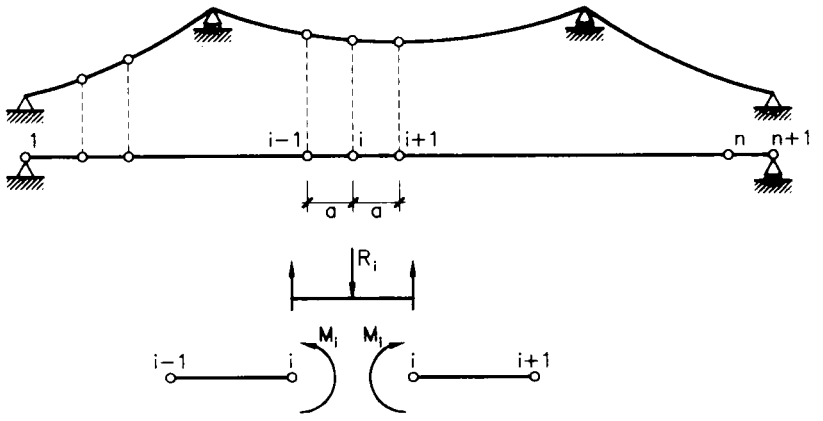

FIGURE 4 Discretization of suspension bridge.

TABLE 4 Expression for Matrix $\underline{\underline{K_g}}'$ for Single-Span Bridge

$\underline{\underline{K_g}}'/n^3$		w_1	w_2	w_3	w_4	w_5	...	w_{n-2}	w_{n-1}	w_n	w_{n+1}
		1	2	3	4	5	...	n-2	n-1	n	n+1
w_1	1	α^2	$-2\alpha^2$	α^2	0	0	0	0	0	0	0
w_2	2	$-2\alpha^2$	$5\alpha^2$	$-4\alpha^2$	α^2	0	0	0	0	0	0
w_3	3	α^2	$-4\alpha^2$	$6\alpha^2$	$-4\alpha^2$	α^2	0	0	0	0	0
w_4	4	0	α^2	$-4\alpha^2$	$6\alpha^2$	$-4\alpha^2$	...	0	0	0	0
...	...	0	0	...	...	...	...	...	0	0	0
w_{n-2}	n-2	0	0	0	0	0	...	$6\alpha^2$	$-4\alpha^2$	α^2	0
w_{n-1}	n-1	0	0	0	0	0	...	$-4\alpha^2$	$6\alpha^2$	$-4\alpha^2$	α^2
w_n	n	0	0	0	0	0	0	α^2	$-4\alpha^2$	$5\alpha^2$	$-2\alpha^2$
w_{n+1}	n+1.	0	0	0	0	0	0	0	α^2	$-2\alpha^2$	α^2

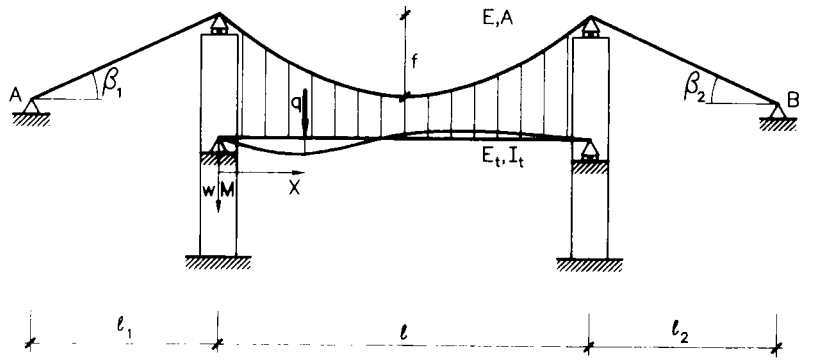

FIGURE 5 Example of single suspended bridge analyzed.

where forces at the ends of the cable have been ignored by assuming that the end displacements are null (matrix $\underline{\underline{C'}}$ should be modified accordingly). If in Equation 12 only first-order terms are retained and cable flexibility is neglected,

$$\mathbf{a}'' \cdot \mathbf{d}' = 0 \rightarrow h' = \frac{\mathbf{a}''^t \cdot \underline{\underline{C'}}^{-1} \cdot \Sigma \mathbf{q}'_i}{\mathbf{a}''^t \cdot \underline{\underline{C'}}^{-1} \cdot \mathbf{a}'} \tag{26}$$

Temperature has not been taken into account in Equation 26. Equations 25 and 26 are the solutions for the inextensible cable. For example, if a load q is uniformly distributed over the whole span, using Equation 26 and Table 1, it is easily derived that $h' = q/q_0$ and $\mathbf{d}' = 0$, which are the expected results.

Simplified Analysis of Suspension Bridges

The stiffness matrices given in Equations 16 and 18 can be directly assembled to solve any kind of structure with a parabolic cable. The external constraints or boundary conditions are introduced in the usual way. The analysis will be correct provided that the forces applied to the cable are vertical. This is the only limitation of the equations.

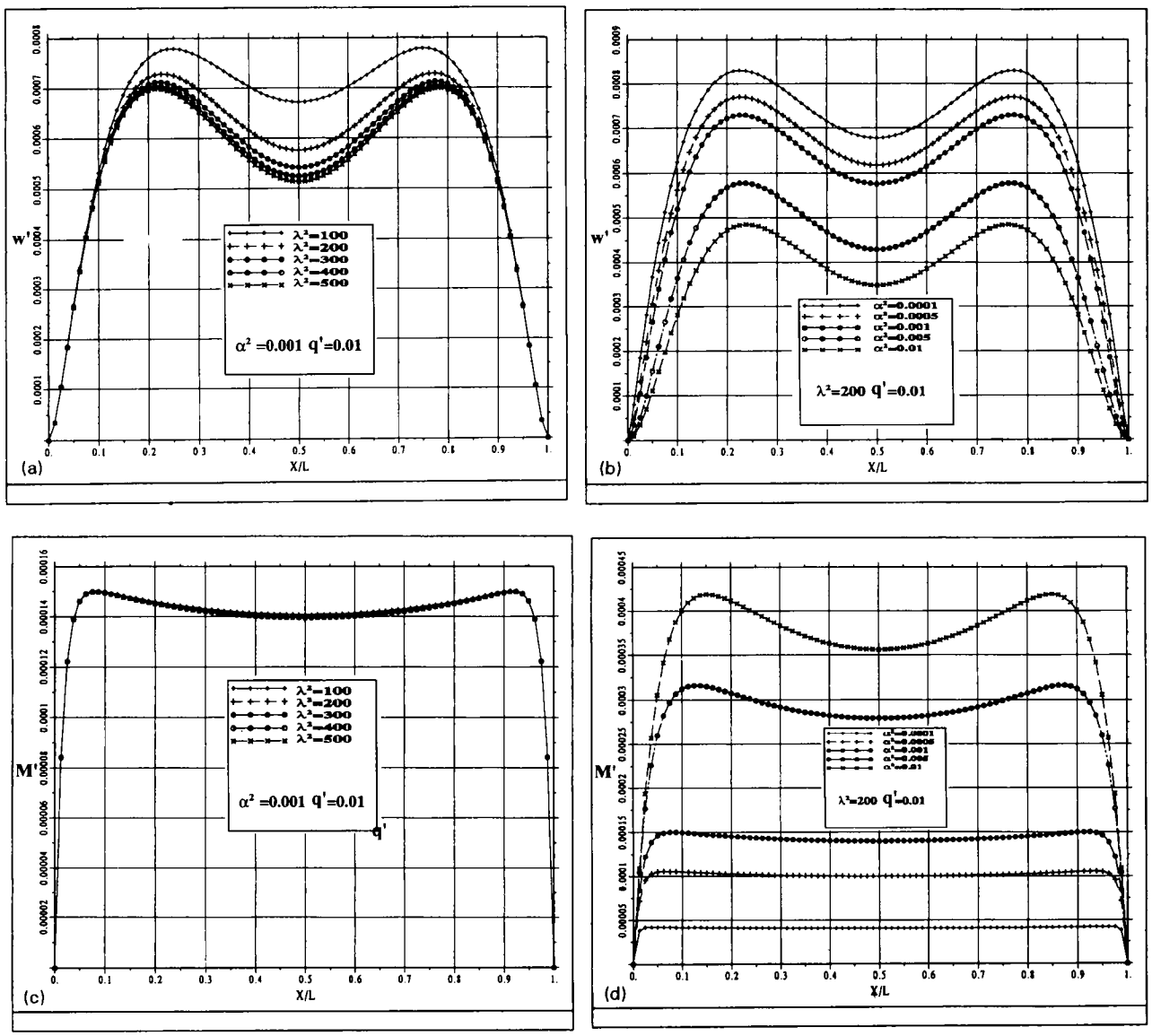

FIGURE 6 Dimensionless displacement under position of concentrated load as a function of (*a*) λ^2, (*b*) α^2; dimensionless bending moment under position of concentrated load as a function of (*c*) λ^2 and (*d*) α^2.

In the case of a suspension bridge with vertical hangers, the problem can be simplified by making the following assumptions:

1. Vertical movements of the cable are the same as those of the beam girder.
2. The hangers remain vertical, so only vertical forces are induced in the cable.
3. The distance between the hangers is assumed to be as small as desired so that vertical interaction forces induced in the cable can be assumed to act at any point of the cable.

These three assumptions are usual in the deflection theory but have also been used in finite element analysis of suspension bridges (*6*). Referring to Figure 4, a very simple analysis can be made by adding the stiffness matrix of the cable to the stiffness matrix of the beam girder.

Any formulation can be used for the determination of the stiffness matrix of the beam. In order to reduce the number of unknowns, in this work the stiffness matrix of the beam has been determined by finite differences. In this way, only vertical movements are taken into account. With reference to Figure 4, flexural mo-

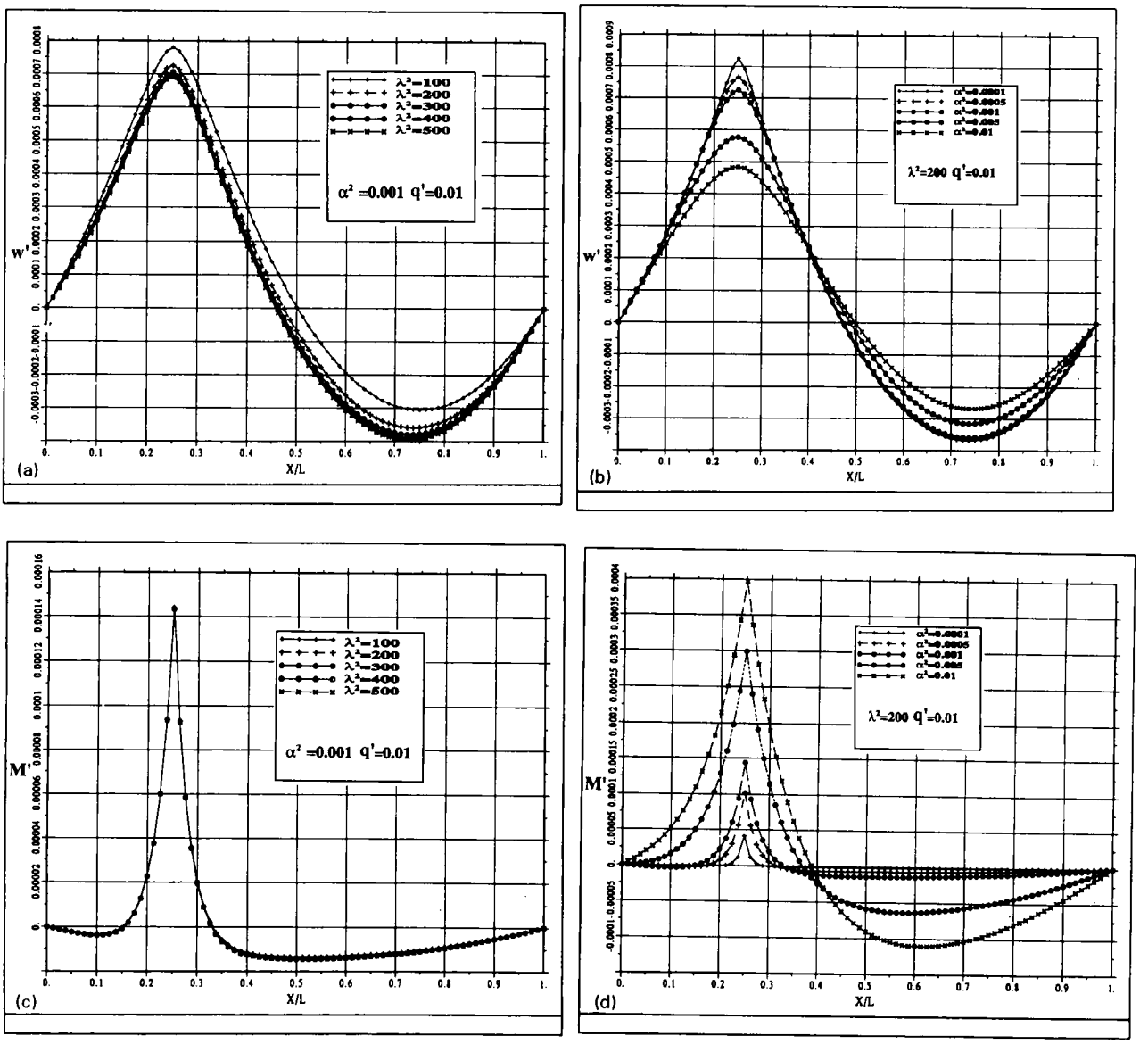

FIGURE 7 Pseudoinfluence line of dimensionless displacement at quarter of span as a function of (*a*) λ^2 and (*b*) α^2; pseudoinfluence line of dimensionless bending moment at quarter of span as a function of (*c*) λ^2 and (*d*) α^2.

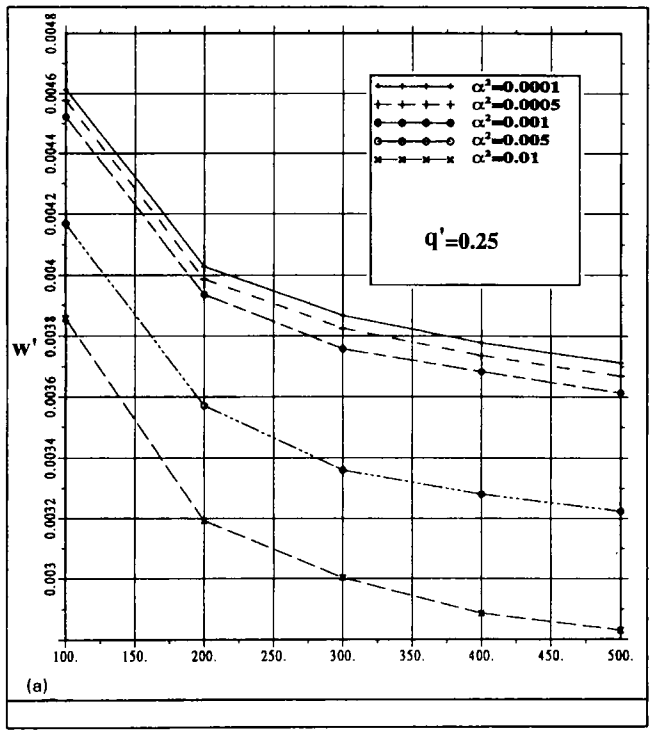

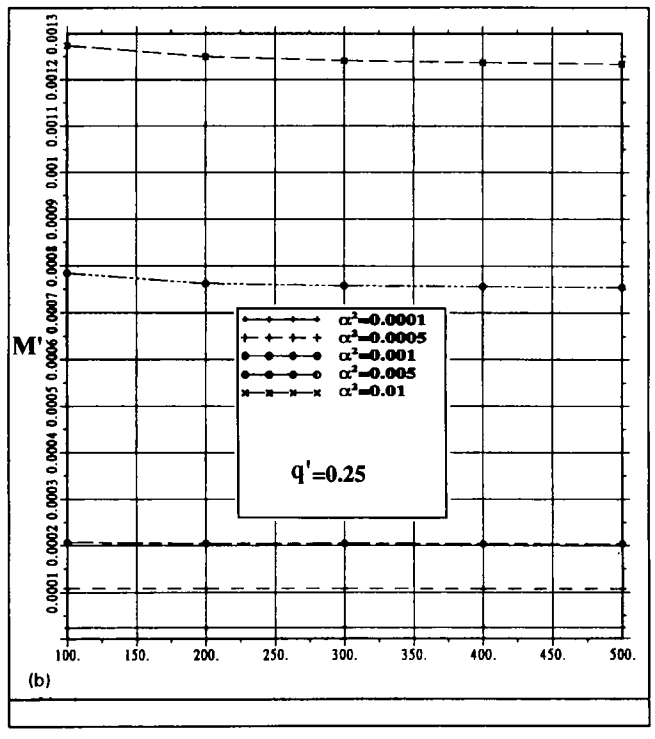

FIGURE 8 (*a*) **Maximum dimensionless displacement and** (*b*) **maximum dimensionless bending moment for arbitrarily located distributed load** $q = 0.25q_0$.

ments are given by the following approximation:

$$\left.\begin{aligned} M_i &= \frac{E_g I_g (w_{i-1} - 2w_i + w_{i+1})}{a^2} \\ R_i &= 2\frac{M_i}{a} - \frac{M_{i+1}}{a} - \frac{M_{i-1}}{a} \\ \underline{\underline{K}}_g \cdot \mathbf{d} &= \mathbf{R} \end{aligned}\right\} \quad (27)$$

where M_i stands for bending moment at node i, w_i for vertical displacement at node i, $E_g I_g$ for the stiffness of the beam, and a for the spacing between points. **R** is the external force vector acting on the beam. The linear stiffness matrix $\underline{\underline{K}}_g$ for the beam can be easily formulated. Assuming that the sum of external forces in the cable plus the external forces in the beam is a vector **P** of external forces in the suspension bridge, the assembly of the global stiffness matrix is obtained straightforwardly by adding the flexural contribution of the beam and the contribution of the suspended cables:

$$[\underline{\underline{K}}_g + \underline{\underline{K}}_c(\mathbf{d})] \cdot \mathbf{d} = \Sigma \mathbf{P} \qquad [\underline{\underline{K}}_g + \underline{\underline{K}}_t(\mathbf{d})] \cdot \Delta\mathbf{d} = \Sigma \Delta \mathbf{P} \quad (28)$$

Again, the expressions are simplified when dimensionless variables are used. The new nondimensional variables introduced are

$$M' = \frac{\mathbf{M}}{q_0 l^2} \qquad \alpha^2 = \frac{E_g I_g}{H l^2} \quad (29)$$

The resultant stiffness matrix $\underline{\underline{K}}_g$ for the beam in dimensionless form is given in Table 4. Only vertical displacements are taken into account.

Examining Equations 19 through 24 and 28 and 29 and Tables 1, 2, and 4, it is seen that the behavior of a given suspension bridge is characterized by only two parameters (λ^2, α^2). The variable λ^2 has already been explained. Parameter α^2 is Steinman's stiffness factor (S^2) (*4*). It measures the ratio between the elastic stiffness of the beam and the gravity stiffness of the cable (*2*). In long-span suspension bridges $\alpha^2 << 1$ (*5*). For example, for the main span of the George Washington Bridge, as originally built (*1*), $\alpha^2 = 8.97 * 10^{-4}$.

Solutions based on the cable inextensibility could be obtained by adding the flexural stiffness matrix to matrix $\underline{\underline{C}}$ in Equations 25 and 26.

Simplified static and dynamic analysis of suspension bridges can be made at a low computational cost with the given expressions. As an example, some dimensionless charts that can be useful in the first phase of design are given below.

Dimensionless Charts

As an example application of the proposed formulation, a single span suspended bridge has been analyzed under

different loading conditions. Two parameters (λ^2, α^2) govern the behavior of the bridge. These parameters can be calculated using only the data of Figure 5. The structural model is also shown in Figure 5. To include the contribution of the backstays in the determination of L_e, Equation 30 should be used:

$$L_e = \left[1 + 8\left(\frac{f}{l}\right)^2\right] l + \frac{l_1}{(\cos \beta_1)^3} + \frac{l_2}{(\cos \beta_2)^3} \qquad (30)$$

Results for the dimensionless displacement and bending moment under the position of a concentrated load ($q' = 0.01$) are shown in Figure 6. The analyses have been performed for a given $\alpha^2 = 0.001$ as a function of λ^2 [see Figure 6(a) for displacement and Figure 6(c) for bending moment], and for a given $\lambda^2 = 200$ as a function of α^2 [see Figure 6(b) for displacement and Figure 6(d) for bending moment]. These charts are similar to those developed by Jennings (*13*).

The pseudoinfluence line for the displacement and the bending moment at the quarter of span for a concentrated load $q' = 0.01$ are given in Figure 7.

Finally, the maximum displacement and the maximum bending moment obtained for an arbitrarily located distributed load ($0.25q_0$) are shown in Figure 8. The length of the loaded zone and the point of maximum displacement and maximum bending moment have been obtained for every pair λ^2, α^2, performing similar analyses to those shown in Figures 6 and 7.

Some trends of suspension bridge behavior are readily explained in these charts. In particular, it is clearly seen that, in modern suspension bridges, where typically $\alpha^2 << 1$, the stiffness of the beam girder does not contribute to the reduction of the displacements. In the past, this observation led to more flexible beam girders and eventually was one of the causes for the Tacoma Narrows Bridge disaster (*1*).

It is also observed that approximate solutions based in the cable inextensibility ($\lambda^2 \to \infty$) will underestimate the displacements in practical cases. However, as shown in Figures 6(c), 7(c) and 8(b), bending moments are not dependent on λ^2, so solutions based on the cable inextensibility will give very accurate results. Interpreting a solution due to Jennings (*13*), the bending moment under the position of a concentrated load q' could be obtained as follows:

$$M' = q' \frac{\alpha}{2} (1 - 3\alpha) \qquad (31)$$

which is approximately correct for every position of the load. As it can be seen, Equation 31 is in close agreement with Figure 6(c) and (d).

Conclusion and Future Work

The objective of this paper has been to introduce a simple numerical method for the analysis of suspended cables under vertical loads, which can be easily applied to the study of suspension bridges.

Both explicit equilibrium and tangent stiffness matrices for the cable have been derived. The implementation of these stiffness matrices in a general computer program for the analysis of structures is straightforward. Any planar structure with a parabolic cable can be solved in this manner, provided that the cable is only subjected to vertical loads.

The application of the proposed method to the analysis of suspension bridges is direct and can be simplified using some of the hypotheses of deflection theory (*2–4*). Although any formulation can be used, the flexural stiffness matrix for the beam in this work has been determined by finite differences. This has been done in order to reduce the number of variables, but will also help for the dynamic analyses.

By using dimensionless variables, parametric studies can be executed easily. The influence of every parameter in the equations is observed directly.

Some charts have been given for a single span suspension bridge, and trends of suspension bridge behavior have been discussed. It is hoped that these charts can be useful in the first phase of design as well as in the understanding of suspension bridge behavior.

ACKNOWLEDGMENTS

This work was supported by a grant to the first author from the Comissionats per a Investigació i Recerca, Generalitat de Catalunya.

REFERENCES

1. Buonopane, S. G., and D. P. Billington. Theory and History of Suspension Bridge Design from 1823 to 1940. *Journal of Structural Engineering*, Vol. 119, No. 3, 1993, pp. 954–977.
2. Pugsley, A. *The Theory of Suspension Bridges*. Edward Arnold, 2 ed., 1968.
3. Ulstrup, C. C. Rating and Preliminary Analysis of Suspension Bridges. *Journal of Structural Engineering*. Vol. 119, No. 9, 1993, pp. 2653–2679.
4. Steinman, D. B., *A Practical Treatise on Suspension Bridges*. J. Wiley & Sons, New York, 1953.
5. Irvine, M. *Cable Structures*. M.I.T. Press, Cambridge, Mass., 1981.
6. Abdel-Ghaffar, A. M. Vertical Vibration Analysis of Suspension Bridges. *Journal of the Structural Division*, Vol. 106, No. 10, 1980, pp. 2053–2075.

7. Chaudhury, N. K., and D. M. Brotton. Analysis of Vertical Flexural Oscillations of Suspension Bridges by Digital Computer. *Proc., International Symposium on Suspension Bridges*, Lisbon, 1966.
8. Jennings, A., and J. E. Mairs. Static Analysis of Suspension Bridges. *Journal of the Structural Division*, Vol. 98, No. 11, Nov. 1972, pp. 2433–2455.
9. Arzoumanidis, S. G. and M. P. Bienek. Finite Element Analysis of Suspension Bridges. *Comput. Struct.* Vol. 21, No. 6, 1985, pp. 1237–1256.
10. Cobo del Arco, D. *Static and Dynamic Analysis of Cable Structures*. Doctoral thesis, to be completed in 1996.
11. Crisfied, M. A. *Non-linear Finite Element Analysis of Solids and Structures*, Vol. 1. Wiley, 1991.
12. Wood, R. D., and B. Schrefler. Geometrically Non-Linear Analysis. A Correlation of Finite Element Notations, *International Journal for Numerical Methods in Engineering*, Vol. 12, 1978, pp. 635–642.
13. Jennings, A. Gravity Stiffness of Classical Suspension Bridges, *Journal of Structural Engineering*, Vol. 109, No. 1, Jan. 1983, pp. 16–36.